PEP-162

SOLENOID DETECTORS FOR $e^+e^- \to \mu^+\mu^-$ AND OTHER FINAL STATES

W. A. WENZEL

Abstract

Several magnetic detector geometries for $e^+e^- \to \mu^+\mu^-$ are studied. Use of the magnet coil as a radiator is considered as a way of building a compact field detector for hadron, photon, electron, and muon physics. The usefulness of e^+e^- elastic scattering to normalize $\mu^+\mu^-$ rates under different conditions of beam polarization is emphasized. Toroidal and solenoidal muon detectors are compared.

A. Introduction

There are several reasons why the study of $e^+e^- \to \mu^+\mu^-$ needs a detector that measures more than this process alone. First, although the $\mu^+\mu^-$ final state is extremely rich in terms of the number of fundamental parameters that can in principle be measured (e.g., coupling constants and intermediate boson mass), untangling these requires careful relative normalization during runs with different beam conditions (i.e., energy and beam polarization). The measurement of at least one parameter ($g_V^e\, g_V^\mu$) requires a precise absolute measurement of the cross-section. Second, certain backgrounds and systematic effects can be checked if the detector has more than the minimum selectivity. For example, the spectrum and asymmetries of penetrating secondaries can be measured. Third, other physics is also interesting, and can potentially be carried out in parallel during the long runs that will be needed for the weak interaction work.

The simultaneous measurement of e^+e^- elastic scattering seems particularly necessary to the $\mu^+\mu^-$ program. We have therefore considered in this report detectors for which the identification of energetic electrons is an integral part.

B. Parameters of $e^+e^- \to \mu^+\mu^-$

We consider only the lowest order electromagnetic and weak interaction (V,A) terms. We assume that both electron beams are unpolarized, or that one or the other (but not both) is polarized longitudinally (indicated by $\lambda\pm$). Muon helicity is not measured.

Then the most general expression for the cross section is

$$\frac{4s}{\alpha^2}\frac{d\sigma}{d\Omega} = (1+2A)(1+\cos^2\theta) + 4B\cos\theta$$

where (using Mikaelian's[1] notation):

$$A \equiv (g_V^e g_V^\mu \pm \lambda \pm g_V^\mu g_A^e)/e^2(1-M_Z^2/s)$$

$$B \equiv (g_A^e g_A^\mu \pm \lambda \pm g_V^e g_A^\mu)/e^2(1-M_Z^2/s)$$

Measurement of σ over a range of angles determines two parameters only (A,B) for a given running condition (s, λ constant). The two terms are orthogonal in $\cos\theta$. For a symmetric detector their values and errors fully describe a given measurement.

For the measurement of interesting quantities we note:

1. The s dependence of the coupling constants gives the intermediate boson mass^2 (M_Z^2).
2. With no polarization of the beam $g_A^e\, g_A^\mu$ (= g_A^2) can be determined from a simple asymmetry measurement: $A_0\ (\cos\theta) \approx 4B\ \cos\theta/(1+\cos^2\theta)$.
3. With no polarization $g_V^e\, g_V^\mu$ (= g_V^2) requires an absolute measurement. This requires that either:
   a. Absolute detector efficiency and luminosity are known, or
   b. Detector efficiency for $\mu^+\mu^-$ relative to that for some other process that can be calculated is known. The best candidate for such a process is $e^+e^- \to e^+e^-$. This should be measured at large angles and over a range of angles to avoid the extreme sensitivity of cross section to scattering angle and beam direction. Hence, a good electron detector within the muon detector is desirable. If elastic scattering violates QED, the experiment is, of course, even more interesting, although there may be simpler ways to measure the latter process.
4. With polarization, the term $g_V^e\, g_A^\mu$ is determined from the difference of asymmetries measured with and without polarization or with polarizations of opposite sign. A serious systematic problem is the necessary change of beam direction (vertically) in order to effect longitudinal polarization.[2]

5. In order to detect a violation of μ-e universality we need the difference of the two V-A interference terms. For this, $g_V^\mu g_A^e$, must be determined separately from the term discussed in 4. This is obtained from the relative difference of the total rate with and without polarization. Absolute normalization is not required, but relative normalization with strongly variable beam conditions is necessary.

Therefore, we believe that a good detector for e^+e^- elastic scattering is desirable if not essential for most of the $\mu^+\mu^-$ physics.

For a detector with azimuthal and polar symmetry the relative effectiveness in the measurement of Rate ($d\sigma/d\Omega \propto 1 + \cos^2\theta$) and asymmetry ($A \propto \cos\theta/(1 + \cos^2\theta)$) can be defined unambiguously in terms of inverse integrated luminosity to achieve a given precision, i.e.,

$$\epsilon_R \equiv \int_{detector} d\sigma \Big/ \int_{4\pi} d\sigma = \frac{1}{4}\left[3(\cos\theta_{min} - \cos\theta_{max}) + \cos^3\theta_{min} - \cos^3\theta_{max}\right]$$

$$\epsilon_A \equiv \int_{det.} A^2 d\sigma \Big/ \int_{4\pi} A^2 d\sigma = \frac{\cos\theta_{min} - \cos\theta_{max} - \tan^{-1}\cos\theta_{min} + \tan^{-1}\cos\theta_{max}}{1 - \pi/4}$$

Figure 1[(3)] shows how this varies with $\cos\theta_{min}$ for $\theta_{max} = \pi/2$. The vertical marks are for two detector designs considered in the next section. The curves corresponding to ϵ_R and ϵ_A give the performance for g_V^2 and g_A^2 respectively. Interference terms $g_A g_V$ fall somewhere in the included area.

From the Figure we see that asymmetry measurements benefit more than rate measurements from acceptance at a small polar angle. At 30-degrees the running time for a given precision in asymmetry would be only 40 per cent greater than for a 4π detector (if this could be built).

C. Detector for Other Physics Too

We have examined two kinds of muon-electron detectors, one of which would preserve the possibility of doing other physics by providing a high resolution low density charged particle detector as well as a shower detector inside the magnetic field volume.

In addition to $e^+e^- \to e^+e^-$ are discussed above, we note:

1. Events with an energetic electron and muon in the final state could indicate the production of the heavy leptons.
2. Hard hadrons (the charge but not the type is determined) and γ-rays can

be identified by elimination of electrons and muons. These can reveal fundamental properties and form factors of em and strong interactions.

3. Muons can arise in the decay of charmed particles.
4. Vertices are well defined, so strange particles can be studied.
5. Correlations in charged and neutral (soft) multiparticle final states have been studied particularly in connection with Group A's MINIMAG SPEAR proposal. It is possible that our detector could do some of the same kind of work; however, very careful attention to the relative sensitivity of the γ-ray detector is needed.

Figures 2 and 3 shows detectors suitable for hadron and γ-ray as well as muon-electron detection. The lead-scintillator sandwiches include fourteen 0.2 radiation length lead sheets. The copper magnet coils provide ten layers of 1 radiation length (radially) each. The inner charged particle detectors are high resolution drift chambers that can operate symmetrically in high magnetic fields. The chamber design would follow that proposed by Group A for MINIMAG.

Use of the magnet coil in this hybrid way permits high field to be obtained in a small device with relatively low power. The 15-kg field requires about 1.5 MW; this can be reduced at the expense of field uniformity by bringing the pole-tips closer together at small radius.

Figure 4 shows an end view of the detector(s). The return yoke, which provides most of the muon filtering, is adjusted to provide polar equalization of the muon path length in the absorber. The iron surfaces can be torch cut.

Cost of the raw material for the spectrometer(s) [omitting the wire chambers, scintillators and electronics] is approximately as follows:

Phototubes		
	5-in., 50 x $500	$ 25K
	2-in., 150 x $100	15
Steel	200T @ $0.2/lb.	40
Copper	10T @ $2/lb	20
		$100K

This estimate, of course, ignores the cost of development, fabrication and other things that are omitted.

The scintillators in the radiator (see Figure 5) are made up of flat, long strips that can be slid into the annular slots between the assembled coil layers. They are tapered on the ends. No gluing is necessary, provided that the forms for scintillator fabrication can be long enough. The only light guides are cylinders of lucite to let the phototubes be located outside the pole-tips.

The scintillators are viewed from both ends. With standard circuitry they can obviously be used to provide fast timing information for $\mu^+\mu^-$ and e^+e^- final states.

Figure 6 shows the momentum resolution as a function of magnetic field strength, momentum and inner chamber resolution. The muons are measured better than the hadrons and electrons by using an additional chamber at 1 meter radius. We would do still better by using the deflection in the return yoke. This effect is not inlcuded in the resolution estimates. In the region of interest the error for the inner detector is dominated by chamber resolution. The error in the use of the chamber at 1 meter is dominated by coulomb scattering.

For such a detector we conclude the following from Figure 6:

a) Even with spark chambers ($\delta_0 \approx 0.3$ mm), a muon momentum resolution of 17 per cent is obtained for 15 GeV at 1.5 tesla. For SPEAR at 3 GeV, the resolution would be 10 per cent.

b) With 0.1 mm drift chamber resolution at 1.5 tesla, a 15 GeV electron or hadron would be measured to 20 per cent, while a 3 GeV muon, electron or hadron is measured to 4 per cent, provided that the total (distributed) material through the inner detector is substantially less than 0.2 radiation lengths.

D. Iron Balls and Solenoidal Detectors

To select and measure muons of high energy, magnetized iron can be very useful. If we give up hadron physics, the power requirements are dramatically reduced. Figure 7 shows how toroidal or cylindrical geometry can be used with magnetic deflection in solid iron. Measurement errors tend to be dominated by coulomb scattering. Spark chamber resolution ($\approx$0.3 mm) appears to be sufficient up to 15 GeV.

To measure e^+e^- events we have included in the relatively field free region a shower detector of $\simeq$10 radiation lengths (radially). We have compared the toroidal and cylindrical geometries for different maximum radii and a polar acceptance from -30 to +30 degrees. We assume, for example, that the transverse dimensions of the experimental area will be limiting. In each case the solenoid will therefore be much heavier than the toroid. For reasonable sizes this is not a severe limitation, however, especially because tolerances on the steel yoke are rather loose. Also the detectors may have to be larger for the solenoid, but in this case the precision needed in the azimuthal measurement is readily achieved using long wires parallel to the beam axis.

For the solenoid the core and yoke dimensions are adjusted so that the field everywhere in the iron is the same (2 tesla). The toroid, also at 2 tesla, presents a spherical outer surface, and the thickness as a function of polar angle is adjusted so that the stopping power is the same in all directions.

The resolution for the measurement of momentum of a single particle is shown in Figure 8. It is energy independent because coulomb scattering dominates. The toroid is generally better than the solenoid. The most important difference is that for the solenoid the resolution goes at $\sin\theta^{-1/2}$. [Note that for the solenoid detector dominated by chamber resolution the momentum resolution goes as $\sin\theta$.] However, two effects have been omitted that make the iron solenoid better than implied in Figure 8. First, measurement on the outside of the return yoke could be used to reduce the error. The deflection of the yoke is about half that in the core, hence a 20 per cent reduction in the overall single particle resolution for the solenoid would be possible. Second, viewed along the beam axis, the muons emerge back to back. This can be used as an additional constraint in the momentum measurement using the solenoid. It is also an important constraint in rejecting background. In the other projection radiative effects destroy the colinearity of the muons. We conclude that there isn't much reason to choose between the solenoid and toroid as far as intrinsic momentum resolution is concerned. There may be some practical problems associated with the alignment of the internal and external chambers. It would appear easier to do this in azimuth than in polar angle. This would tend to favor the solenoid geometry.

Other comparisons of systematic effects can be made. A possible criticism of the solenoid geometry is that the proportion of muons lost from radiative tails depends on polar angle. For a given maximum detector radius this loss is on the average larger for the solenoid than for the corresponding toroid. To minimize such losses, only a reasonable fraction, say less than half, of the energy should be absorbed in the detector. We note also that energy loss by muons is not charge symmetric. The effect, at a level of $\approx$1/3 per cent, has been both observed[4] and explained[5]. In our present case, however, each $\mu^+\mu^-$ event requires the detection of both muons with a highly symmetric detector. Hence, there would be no important contribution to systematic asymmetry backgrounds from the effects discussed above.

There are also compensations for the dependence on polar angle of the path length in the iron. The small angle backgrounds are more likely to be asymmetric; hence stronger filtering is justified. An extreme example is e^+e^- elastic scattering. It is therefore appropriate also that the effective thickness of the electron detector varies as $\sin\theta^{-1}$ as is implied in Figures 2,3 and 7.

A more serious systematic effect can arise in the asymmetry of backgrounds for $\mu^+\mu^-$ events when the signs of the charges are reversed. Figure 9 shows the topology of $\mu^+\mu^-$ vs. $\mu^-\mu^+$ events in the toroidal and solenoidal geometries. In both cases both muons from events with a given θ, ϕ production go through different parts of the detector when the charges are reversed. Because background variation with polar angle is more to be expected than variation with azimuthal angle, the toroidal geometry is more likely to get into trouble. It is easier to build a device that is axially symmetric in detection efficiency. Detailed axial symmetry is not necessary for the solenoid. As long as the detection (and background) symmetry is even in ϕ (i.e. with respect to the vertical plane containing the beam) no polar asymmetry is introduced. Note that both transverse polarization and vertical beam steering to produce longitudinal polarization also will produce effects that are even in ϕ and will therefore not lead to a systematic polar asymmetry for the solenoid.

For the toroid there are more likely to be problems, because background can depend on $\cos\theta$ (or $\sin\theta$) so that $\mu^+\mu^-$ and $\mu^-\mu^+$ events are detected with different efficiencies. It is obviously desirable to reverse the magnetic field for half the running. This should be done for any detector, because it interchanges the topologies that we are concerned with. Limitations of this procedure are that the field may not reverse perfectly, and also, that not everything else stays the same, e.g., there are more negative electrons and positive protons in the backgrounds of our world. The best detector is as symmetric as possible before the magnetic field is reversed.

We conclude that the solenoid geometry is more likely to avoid systematic asymmetries. For the cost of about a megawatt of power (we have not considered superconductivity) a compact design which measures processes other than $e^+e^- \rightarrow \mu^+\mu^-$ seems to be a worthwhile development.

References

1. Karnig O. Mikaelian, "Testing Weak Neutral Currents in Longitudinally Polarized Colliding Beams." Case Western Reserve (Internal Report). Also E. A. Paschos, 1974 Summer Study - first week review.
2. R. Schwitters, and B. Richter, PEP-87.
3. For transverse beam polarization ε_R is unchanged, but ε_A is modified. The limiting case for $P_t^+ P_t^- = 1$ is $\varepsilon_A = \cos^2\theta_{min.}$ (See Figure 1)
4. A. R. Clark, R. C. Field, H. J. Frisch, W. R. Holley, R. P. Johnson, L. T. Kerth, R. C. Sah, and W. A. Wenzel, Physics Letters 41B, 229 (1972).
5. J. D. Jackson, and R. L. McCarthy, Physics Review B6, 4131, (1972).

FIGURE 1

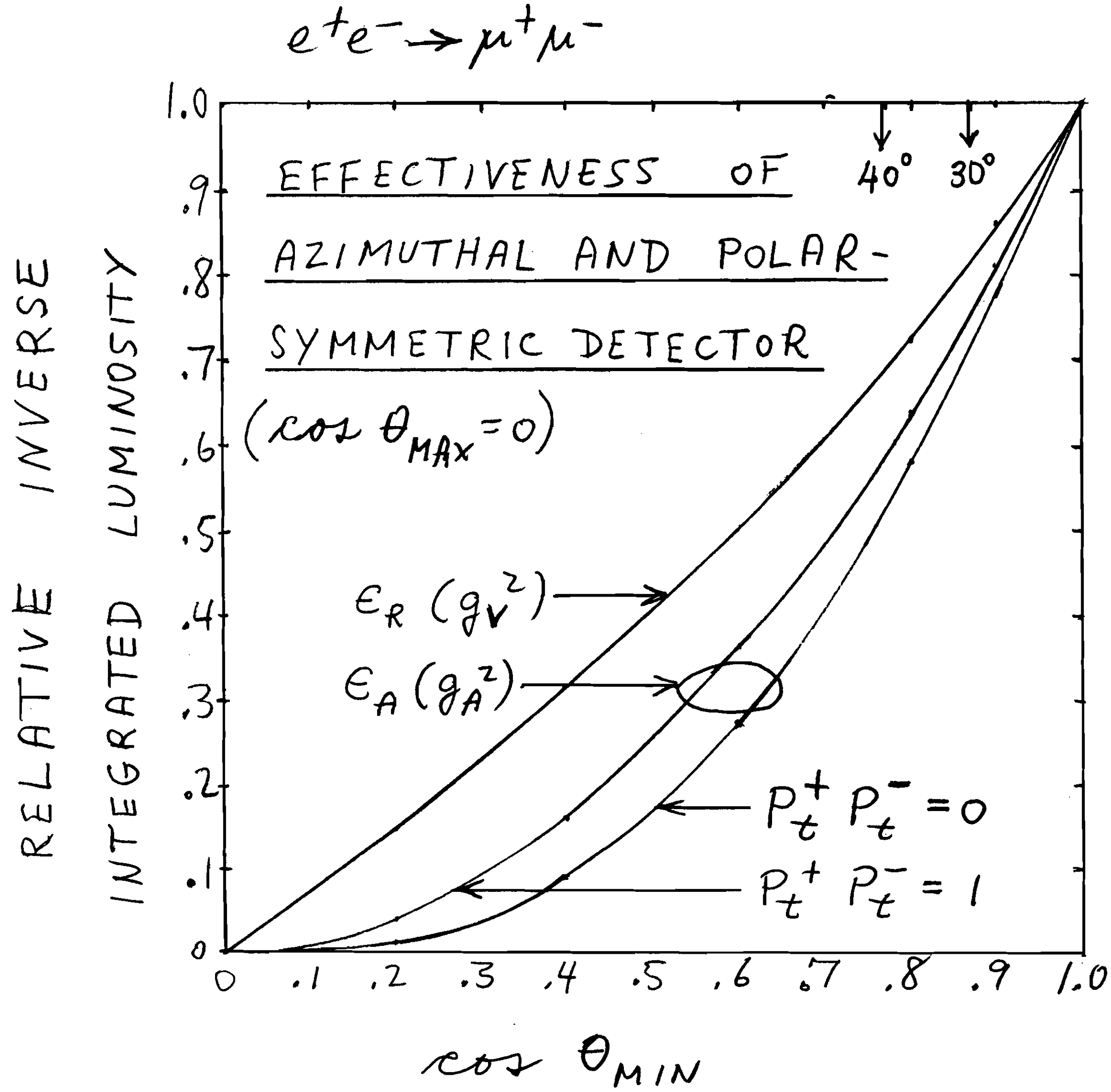
e+e- → μ+μ-
EFFECTIVENESS OF
AZIMUTHAL AND POLAR-
SYMMETRIC DETECTOR
(cos θMAX = 0)
40°
30°
εR (gV²)
εA (gA²)
Pt+ Pt- = 0
Pt+ Pt- = 1
RELATIVE INVERSE
INTEGRATED LUMINOSITY
cos θMIN
0
.1
.2
.3
.4
.5
.6
.7
.8
.9
1.0

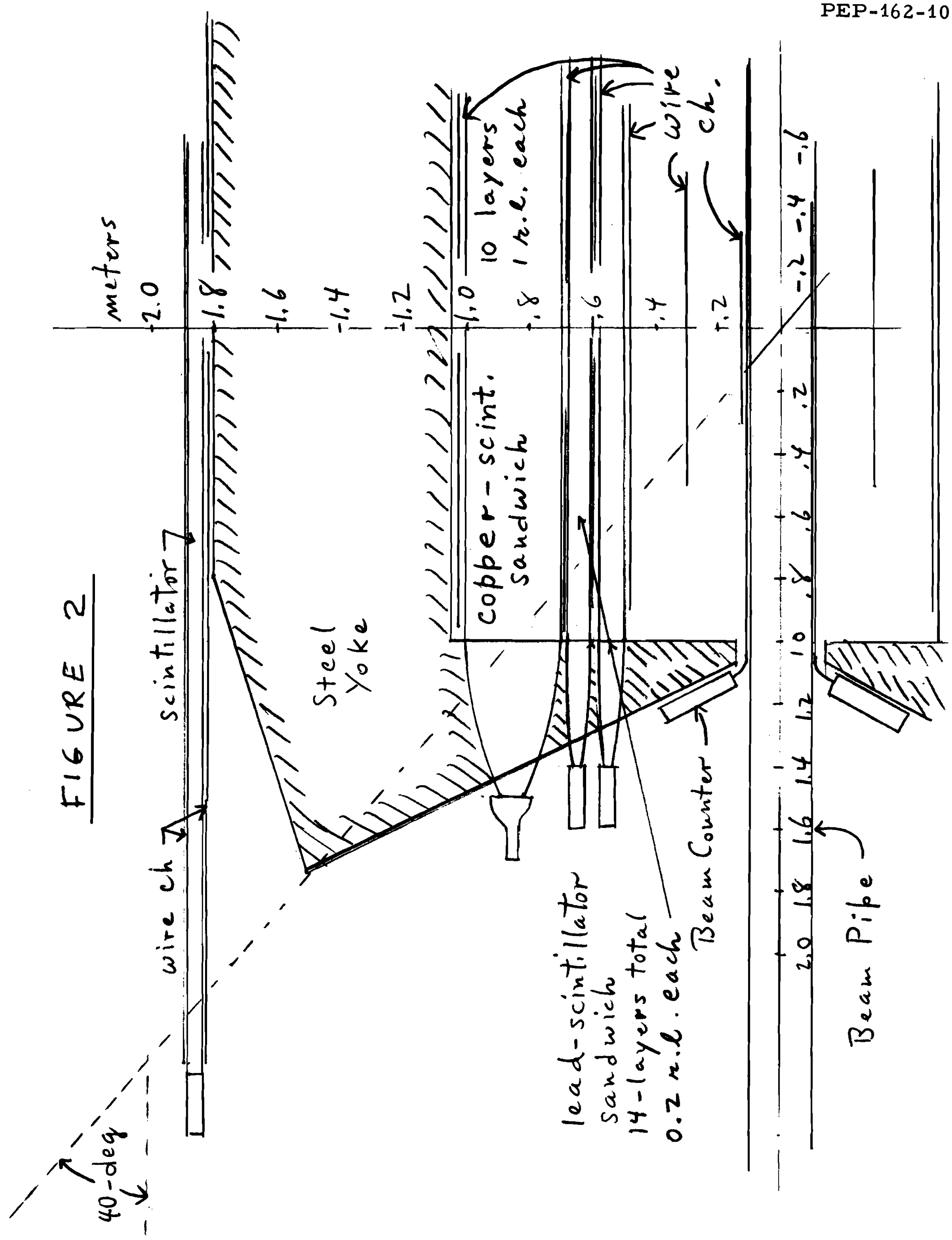
meters
2.0
1.8
1.6
1.4
1.2
1.0
.8
.6
.4
.2
-.2
-.4
-.6
10 layers
1 r.l. each
wire
ch.
copper-scint.
sandwich
Steel
Yoke
scintillator
wire ch
40-deg
lead-scintillator
sandwich
14-layers total
0.2 r.l. each
Beam Counter
Beam Pipe
.2 .4 .6 .8 1.0 1.2 1.4 1.6 1.8 2.0

FIGURE 2

FIGURE 3

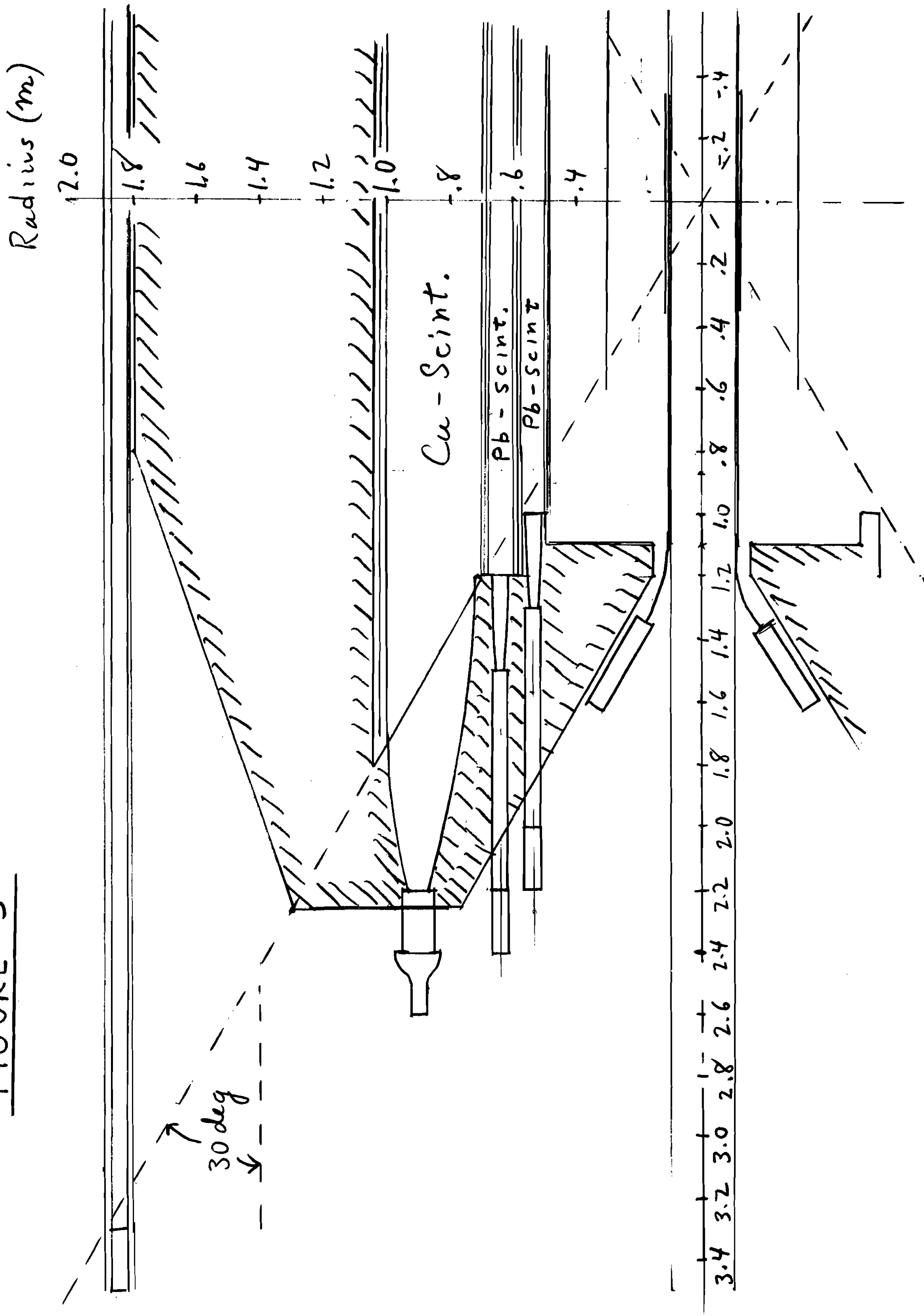
Radius (m)
2.0
1.8
1.6
1.4
1.2
1.0
.8
.6
.4
Cu-Scint.
Pb-scint.
Pb-scint
30 deg
.4
.2
.2
.4
.6
.8
1.0
1.2
1.4
1.6
1.8
2.0
2.2
2.4
2.6
2.8
3.0
3.2
3.4

FIGURE 4

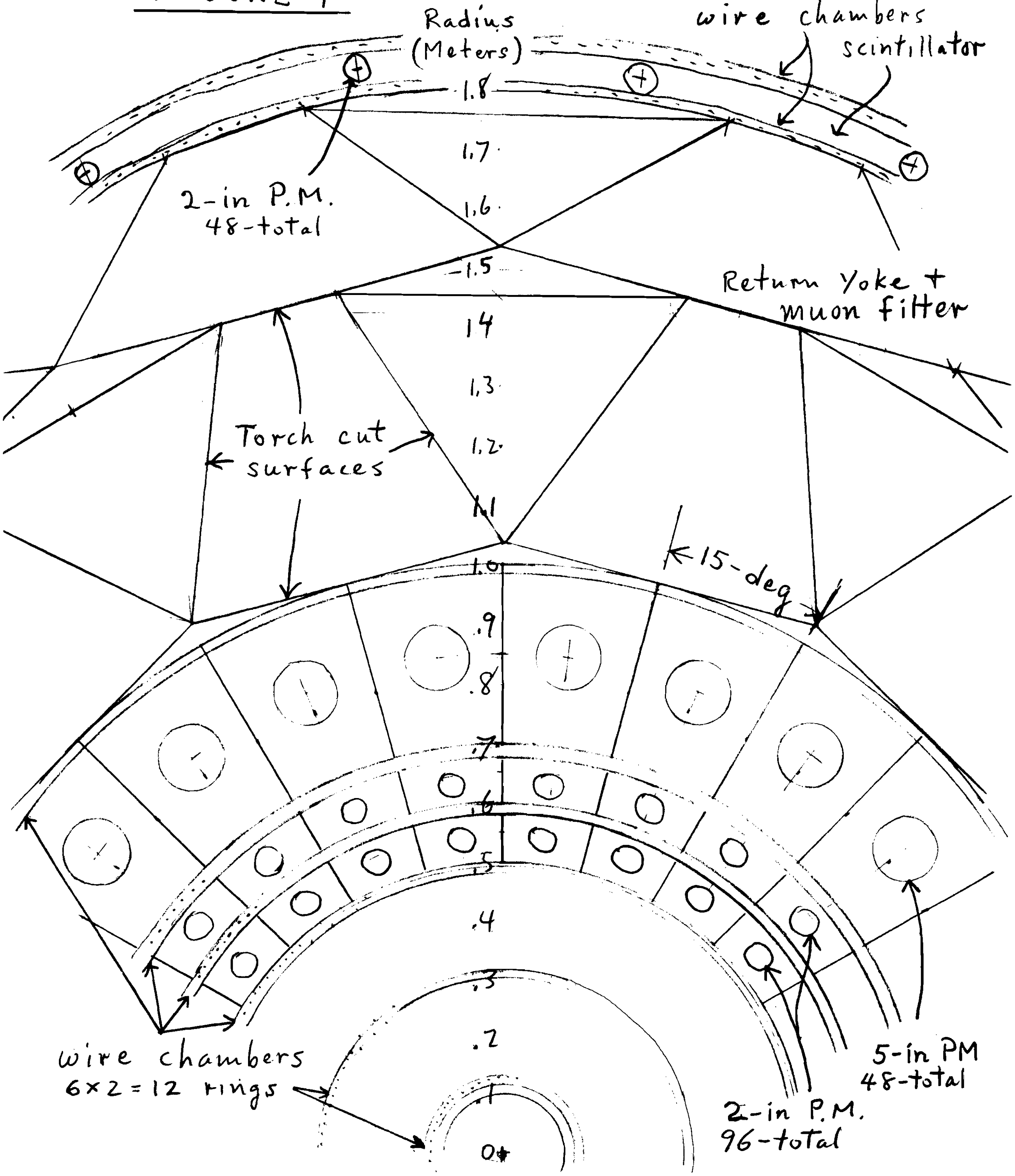

Radius (Meters)
wire chambers
scintillator
1.8
1.7
1.6
1.5
14
1.3
1.2
1.1
1.0
.9
.8
.7
.6
.5
.4
.3
.2
.1
0
2-in P.M. 48-total
Return Yoke + muon filter
Torch cut surfaces
15-deg
wire chambers 6×2=12 rings
2-in P.M. 96-total
5-in PM 48-total

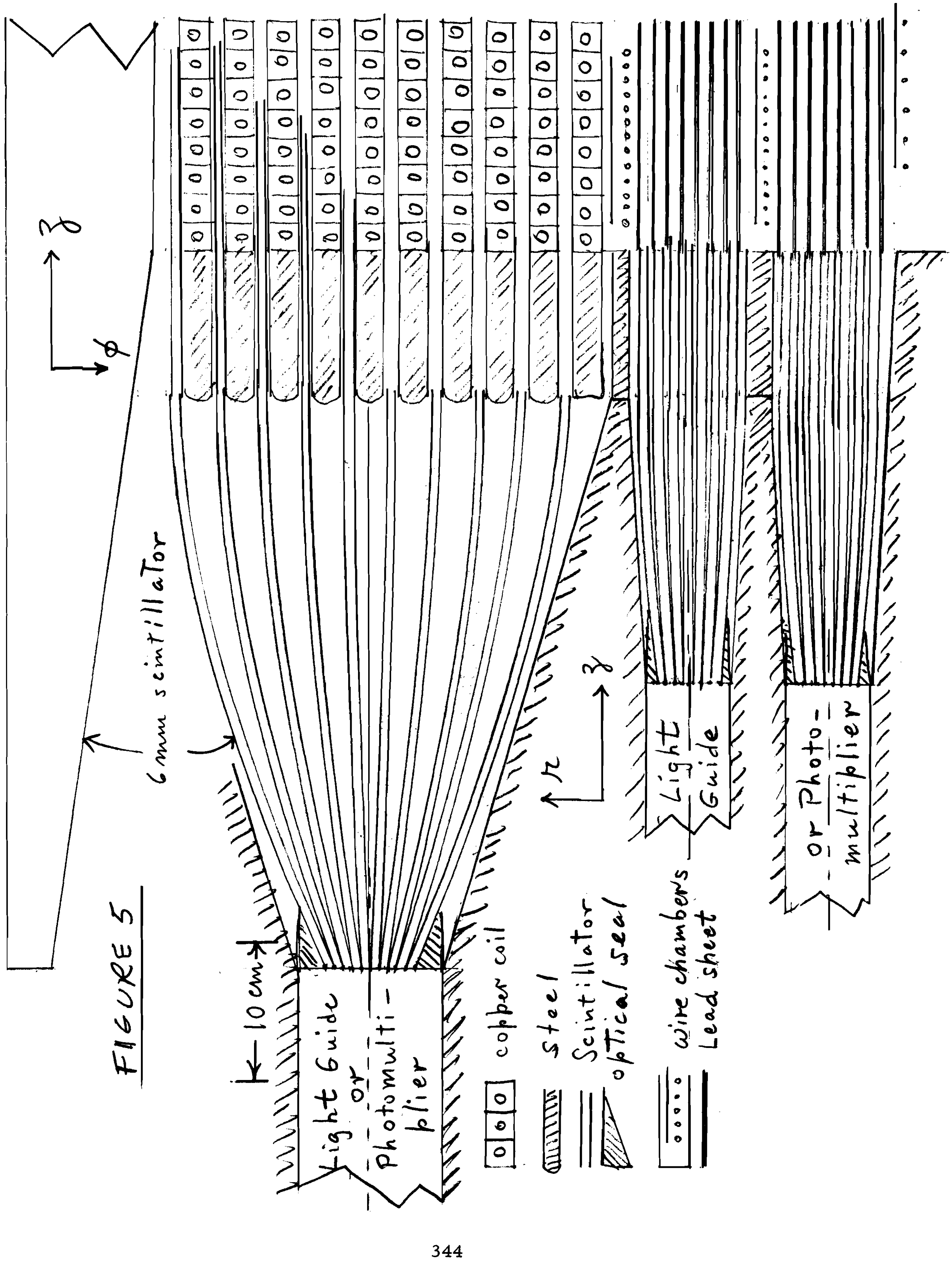
6 mm scintillator
10 cm
Light Guide or Photomultiplier
copper coil
steel
Scintillator
optical seal
wire chambers
Lead sheet
Light Guide
or Photo-multiplier
z
φ
r

FIGURE 5

FIGURE 6

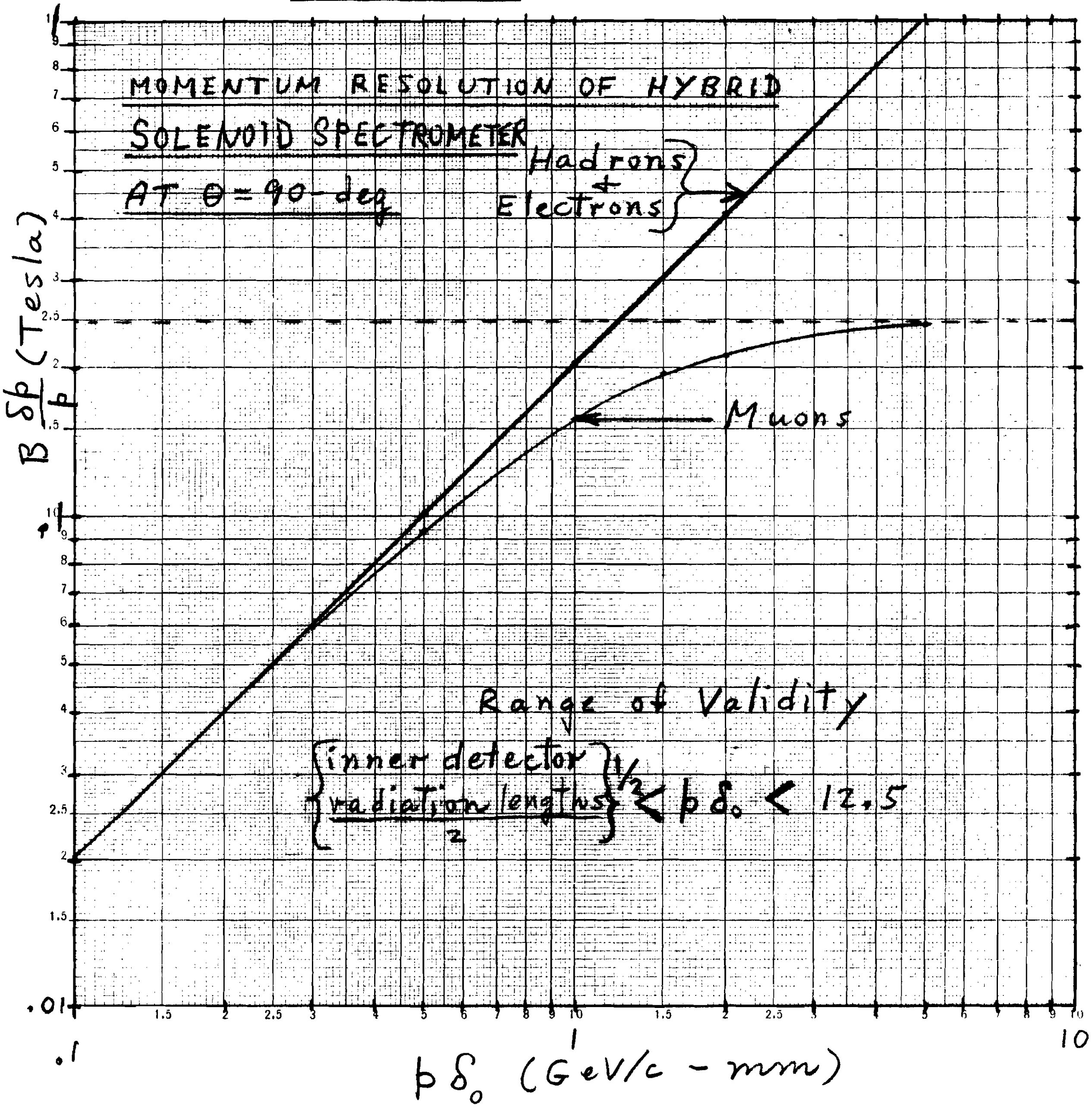
MOMENTUM RESOLUTION OF HYBRID
SOLENOID SPECTROMETER
AT θ = 90-deg
Hadrons + Electrons
Muons
Range of Validity
{inner detector radiation lengths / 2}^1/2 < pδ₀ < 12.5
B δp/p (Tesla)
pδ₀ (GeV/c - mm)
.01
.1
1
10

FIGURE 7

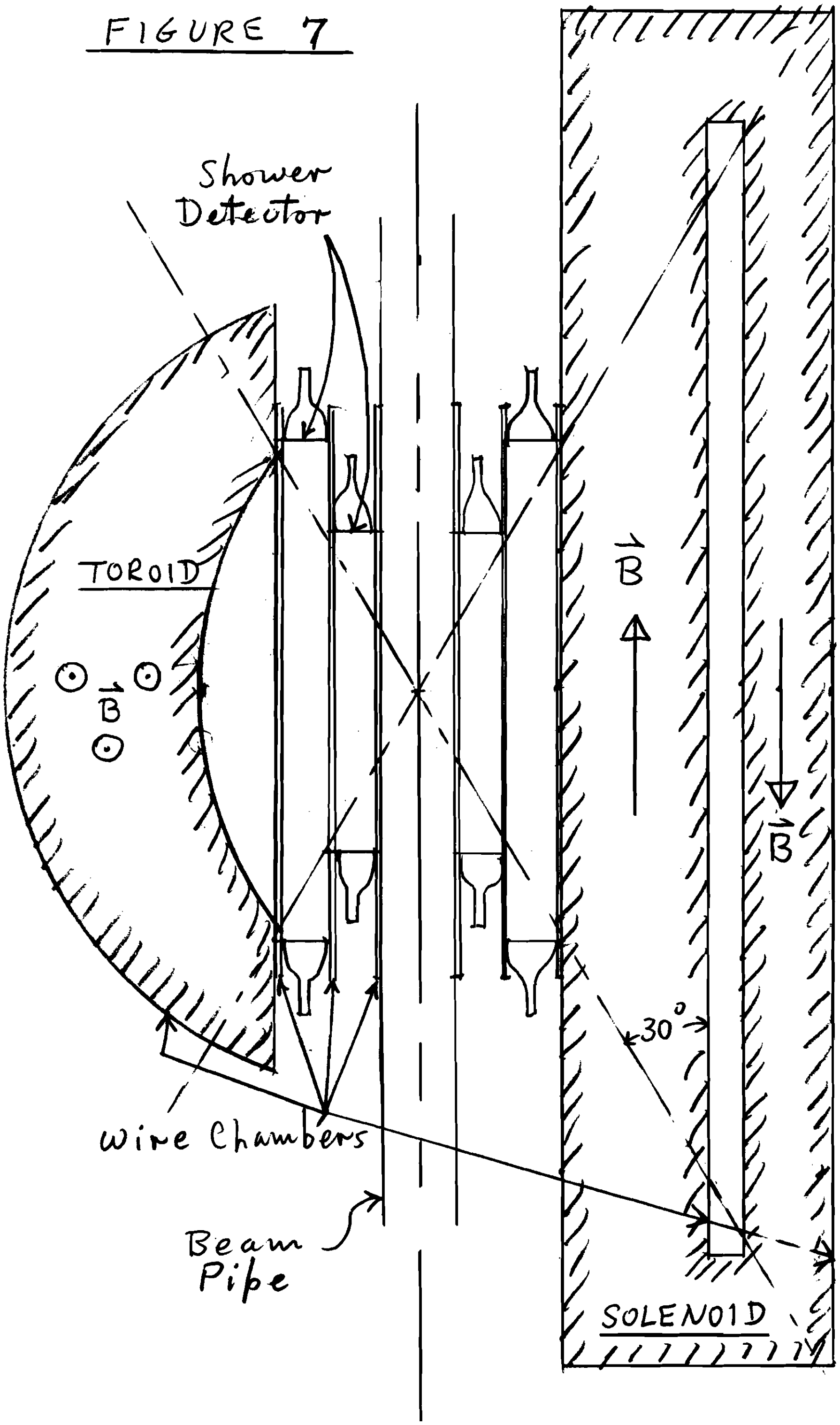
Shower
Detector
TOROID
B
B
B
30°
B
Wire Chambers
Beam
Pipe
SOLENOID

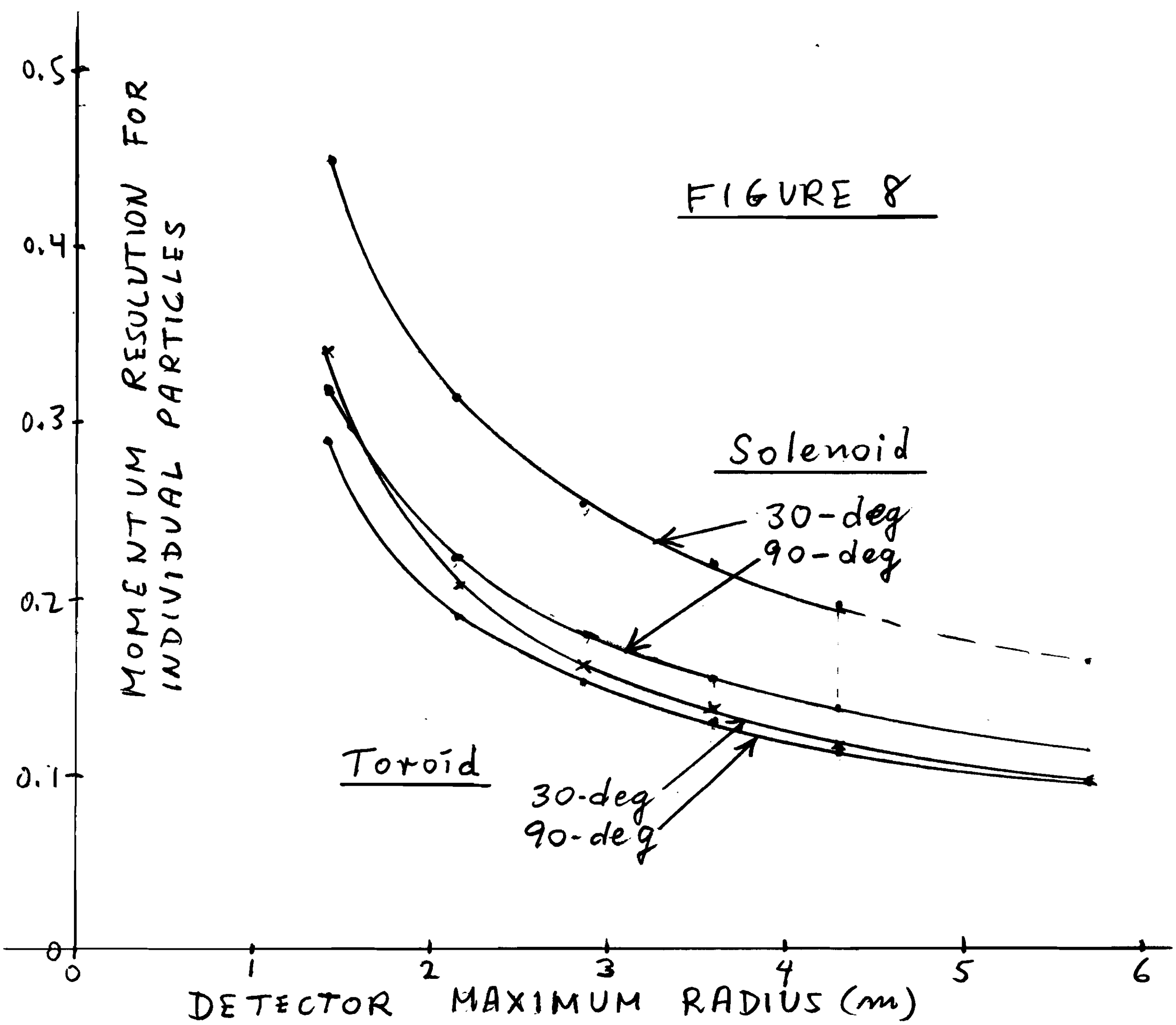
FIGURE 8
MOMENTUM RESOLUTION FOR INDIVIDUAL PARTICLES
0.5
0.4
0.3
0.2
0.1
0
Solenoid
30-deg
90-deg
Toroid
30-deg
90-deg
0
1
2
3
4
5
6
DETECTOR MAXIMUM RADIUS (m)

FIGURE 9